Journal of Materials Chemistry B

PAPER

View Article Online
View Journal | View Issue

Cite this: J. Mater. Chem. B, 2015, 3, 562

Post-infiltration and subsequent photo-crosslinking strategy for layer-by-layer fabrication of stable dendrimers enabling repeated loading and release of hydrophobic molecules†

Yue Wang,[a] Qi An,*[b] Yong Zhou,[a] Yue Niu,[a] Raheel Akram,[a] Yihe Zhang[b] and Feng Shi*[a]

Received 12th October 2014
Accepted 7th November 2014

DOI: 10.1039/c4tb01688b

www.rsc.org/MaterialsB

The layer-by-layer (LbL) technique has been intensively investigated as a straightforward method for the incorporation of drug molecules or other bioactive species, enabling retarded release in drug delivery devices, in bioactive interfaces, in tissue engineering, and in regenerative medicine. The preparation of crosslinked LbL multilayers with embedded drug reservoirs for delayed release remains a challenging task, however. In the present study we have developed a method for the simultaneous utilisation of covalent interlayer linkages and drug reservoirs that can hold model drug molecules. A strategy of post-infiltration of photoactive bifunctional small molecules followed by UV irradiation has been employed for crosslinking the LbL multilayers, incorporating poly(amido amine) (PAMAM) molecules, which serve as a drug reservoir. The covalent linkage significantly alters the release profile of the model drug from the multilayers, with retarded release of hydrophobic molecules from a solvent, and enabling the loaded multilayers to withstand rinsing with 75% ethanol, the most commonly used sterilization procedure.

1. Introduction

The layer-by-layer (LbL) technique offers a simple method for the incorporation of drug molecules or bioactive species, allowing retarded release from drug delivery devices and bioactive interfaces in tissue engineering and regenerative medicine.[1–6] During recent decades the LbL technique has been developed to improve retarded release. Among the developments, the formation of covalent linkages between adjacent layers has been shown to be an effective method for stabilizing the LbL multilayers, allowing them to be used in biologically relevant environments over prolonged periods.[7] For example, Caruso *et al.* have described the crosslinking of LbL multilayers by the introduction of glutaraldehyde and have investigated the loading capacity of the assembled dendrimer.[8] Another improvement in controlling retarded release from LbL multilayers has been to include larger amounts of cargo, by using specific building polymers allowing the incorporation of more binding sites,[9] by the construction of thicker films,[10] or by use of microgels or nanoparticles as drug reservoirs.[11–13]

In particular, a number of drug release mechanisms of LbL assembled multilayers have been demonstrated,[14–17] allowing the loading and release behavior to be repeated over a series of cycles, despite the fact that LbL-assembled multilayers are normally not durable under extreme conditions of pH or ionic strength. However, the incorporation of these improvements has been a challenging task. The covalent crosslinking of multilayers often requires the multilayers to have specific reactive species built in.[8,18–25] In addition the introduction of reactive functional groups may significantly decrease the binding sites in the multilayers, damaging the electrostatic micro-environment necessary for the incorporation of charged cargo, or impose additional difficulties in the fabrication of the microgel used as a micro-scale drug reservoir in the multilayers. The development of strategies for simultaneously achieving covalent crosslinking of the multilayers and incorporating drug reservoirs will greatly assist the application of these multilayers in biomedical applications.[7]

A poly(amido amine) (PAMAM) dendrimer is able to accommodate small molecules and nanoparticles in its interior by electrostatic or hydrophobic interaction to form host–guest complexes. PAMAM serves as a hydrophobic micro-container, and offers an effective method of incorporating hydrophobic molecules in a hydrophilic environment.[26–29] The incorporation of PAMAM into LbL multilayers has been widely investigated for achieving retarded release.[30–32] However, most previous studies have designed LbL multilayers using non-covalent interaction,

[a]State Key Laboratory of Chemical Resource Engineering & Key Laboratory of Carbon Fiber and Functional Polymer, Ministry of Education, Beijing University of Chemical Technology, Beijing 100029, China. E-mail: an@cugb.edu.cn; shi@mail.buct.edu.cn
[b]School of Materials Science and Technology, China University of Geoscience (Beijing), Beijing 100083, China. Tel: +86 108 2321797

† Electronic supplementary information (ESI) available. See DOI: 10.1039/c4tb01688b

which may provide insufficient stability. Although the construction of LbL PAMAM multilayers using covalent interactions has been reported, their application in retarded release systems has not been seriously considered,[33–35] and the influence of covalent crosslinking on retarded release in such multilayers requires further study.

In the present study we have developed a method for the simultaneous involvement of covalent interlayer linkages and drug reservoirs for holding model drug molecules. A PAMAM dendrimer with carboxylic terminal groups has been used as a building unit, both for the multilayers and the drug reservoir. A strategy described as *post-infiltration followed by photochemical crosslinking* has been used for the formation of covalent interlayer linkages between the multilayers. In the initial step this involves the construction of LbL multilayers by a conventional technique. A small bifunctional photoactive molecule, 4,4′-diazostilbene-2,2′-disulfonic acid disodium salt (DAS), was infiltrated into the multilayers, followed by UV-induced photochemical crosslinking. Importantly, the covalent linkage significantly altered the release of the model drug from the multilayers, giving retarded release of the hydrophobic molecules due to its solvency, and enabling the loaded multilayers to withstand rinsing with 75% ethanol, the most commonly encountered sterilization method.

2. Experimental

2.1 Materials and instruments

Poly(allylamine hydrochloride) (PAH, M_w 15 000), poly(amido amine) (PAMAM), and (3-mercaptopropyl)-trimethoxysilane (MPTS) were purchased from Sigma-Aldrich. DAS was obtained from Tokyo Chemical Industry, Japan. Hydrogen peroxide (30 wt%), sulfuric acid, acridine orange (AO), ethanol, and sodium hydroxide were purchased from Sinopharm Chemical Reagent Co. Ltd, (Beijing, China).

UV-visible spectra were obtained using a Hitachi U-3900H spectrophotometer. The surface morphology of the polyelectrolyte multilayers was characterized using atomic force microscopy (AFM; Dimension 3100, Veeco, USA). Photochemical crosslinking was conducted by employing a commercially available 400 W high-pressure mercury lamp. An ultrasonic field was applied using an ultrasonic cleaner at a power of 150 W and frequency 40 kHz.

2.2 The modification of sulfonic groups on the substrate

A self-assembled monolayer of sulfonic acid groups was formed as follows. Firstly, the substrate (quartz, or silicon wafer) was treated with a "piranha" solution H_2SO_4–H_2O_2, 7 : 3 v/v (note that the piranha solution is very corrosive and must be handled with caution), and washed with copious amounts of water. Secondly, the treated substrate was immersed in a solution of MPTS in toluene (1×10^{-5} M) for 12 h, producing a monolayer of mercapto groups; and thirdly, the substrate modified with mercapto groups was treated with a mixture of 30% H_2O_2 and acetic acid (1 : 5 v/v) at 50 °C for 1 h to oxidize the mercapto groups to sulfonic groups.

2.3 Formation of PAH/PAMAM multilayer films

The LbL assembly of PAH/PAMAM multilayers was carried out as illustrated in Scheme 1. Firstly, the quartz substrate modified with sulfonic groups was immersed in aqueous PAH (1 mg mL^{-1}, pH 9.4) for 20 min, washed with pure water and dried under nitrogen. Secondly, the quartz was transferred to PAMAM solution (0.1 M in water, adjusted to pH 7.0 using hydrochloric acid) for 20 min, again washed with pure water and dried under nitrogen. These two cycles were repeated alternately until the desired number of bilayers had been formed. The assembled multilayer was denoted $(PAH/PAMAM)_{7.5}$, in which the outer layer was PAH.

The pH value of PAH in the assembly was maintained at pH 9.4 for the following reason. Under these assembly conditions, the ionization of PAH was relatively low (its p*K*a is 9.7).[36] Since the driving force for the LbL assembly of PAH and PAMAM is mainly electrostatic, more PAH becomes adsorbed on the surface to compensate the surface net charges. In the post-infiltration of DAS at pH 3.8, the acidic conditions will increase the protonation of PAH, generating further positive charges and increasing the adsorption of DAS.

2.4 Photochemical crosslinking of the multilayers and investigation of their stability

The substrate with $(PAH/PAMAM)_{7.5}$ multilayers was immersed in an aqueous solution of DAS (5 mg mL^{-1}) at pH 3.8 for 40 min to give equilibrium distribution. The $(PAH/PAMAM)_{7.5}$ multilayers were irradiated using a 400 W high-pressure mercury lamp at a distance of 20 cm and an intensity of 2.5 mW cm^{-2} for 5 min without filters. To evaluate the stability of the films, the $(PAH/PAMAM)_{7.5}$ multilayers were treated by immersion in a NaOH solution, adjusted to pH 12, for 30 min (Fig. 1).

2.5 The adsorption and release of AO molecules by the multilayers

The multilayers were immersed in an aqueous solution of AO (0.2 mg mL^{-1}) to reach equilibrium absorption. The multilayers loaded with AO were then immersed in 8 mL of a 75% v/v aqueous ethanol solution to release the loaded AO molecules. The absorbance of the multilayers was tested every 2 min during the first 10 min and every 5 min thereafter. Following each characterization the ethanol solution containing released AO molecules was replaced. All the substrates were rinsed following dye loading.

3. Results and discussion

The covalently assembled multilayers incorporating PAMAM were first constructed in a conventional LbL manner, in which PAMAM with carboxyl terminal groups and PAH were assembled on a quartz sheet by electrostatic interaction. A bifunctional photoactive small molecule, DAS, was then infiltrated into the multilayers, followed by UV-induced photochemical crosslinking. The sequential assembly of PAH and PAMAM was monitored by the UV-vis spectrometry (Fig. 1(a)). Absorbance around 200 nm, corresponding to amide bonds, was observed

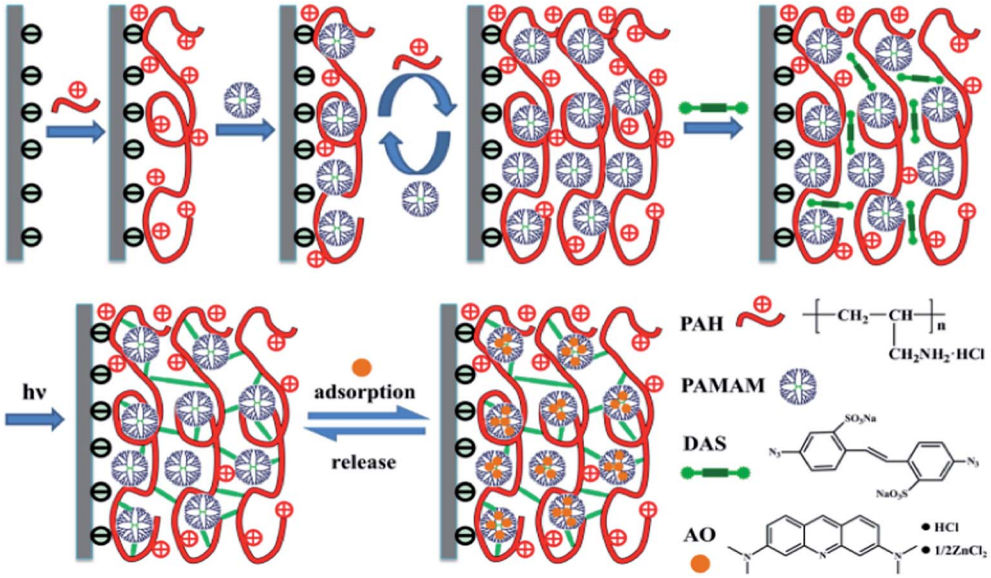

Scheme 1 The stabilization of the PAH/PAMAM multilayers and the infiltration and release of hydrophobic molecules.

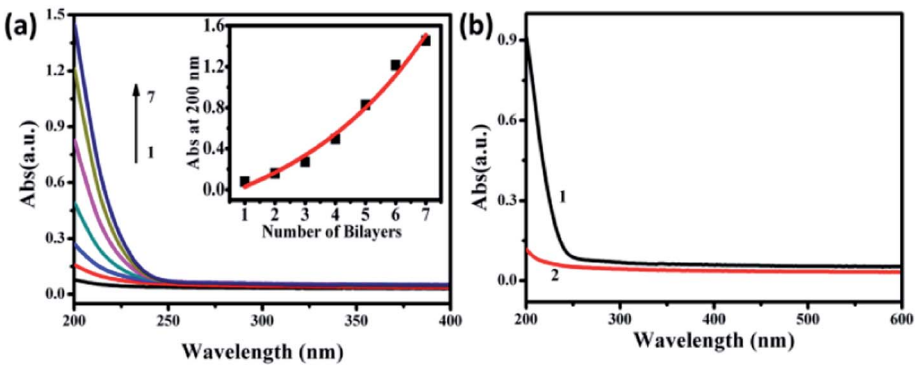

Fig. 1 (a) UV-vis spectra of the sequential assembly of the PAH/PAMAM multilayers; (b) UV-vis spectra of the $(PAH/PAMAM)_{7.5}$ multilayers before (black) and after (red) immersion in NaOH solution at pH 12. The inset in panel (a) is the absorbance at 200 nm for each bilayer. The dots show the measured values and the red line provides guidance for viewing.

in order to follow the assembly of the multilayers. Absorbance to form the PAH/PAMAM multilayer occurred, with an almost linear increase in the number of bilayers. However, in the basic solution (pH 12) the stability of the multilayers was inadequate, and after 30 min immersion the multilayers became disassembled, as shown by the UV-vis spectra (Fig. 1(b)). Disassembly of the multilayers took place since the basic solution deionized the amine groups and thus destroyed the electrostatic attraction between the amine groups in PAH and the carboxyl groups in PAMAM.

In order to increase the stability of the multilayers, photochemical crosslinking of the multilayers using the photoactive molecule DAS was conducted. The infiltration of DAS into the multilayers was monitored using the UV-vis spectra using its characteristic absorbance at 340 nm (Fig. 2(a)). The amount of the absorbed DAS per bilayer was estimated as 0.71 μg cm^{-2} using our previously reported calculation method.[37] In order to improve the efficiency of infiltration, positively charged PAH was assembled on the outermost layer to provide electrostatic interaction with the negatively charged DAS at pH 3.8. Absorbance at around 340 nm increased quickly in the first 300 s and then gradually leveled off. The infiltration became saturated at 1500 s. After saturated absorption of DAS, UV irradiation was conducted at a power of 400 W and a distance of 20 cm. With UV irradiation the characteristic absorbance of DAS decreased over time, accompanied by a concomitant increase in absorbance at around 270 nm and 415 nm. These observations indicated that the azido species in DAS progressively decomposed to form nitrenes, which reacted with adjacent C–H or N–H bonds to form inter- or intralayer covalent linkages.[37–40] The kinetics of the reaction are shown in Fig. 2(b), modeled as an approximate first-order reaction. For peak absorbance (A) at 340 nm, a linear fit of $\ln\{(A_0 - A_{min})/(A_t - A_{min})\}$ *versus* time gave a rate constant (k) of 0.022 s^{-1}, as shown in the inset of Fig. 2(b), in which A_{min} was the minimum invariable absorbance after UV irradiation for 120 s, and A_0 and A_t represented the absorbance at time zero

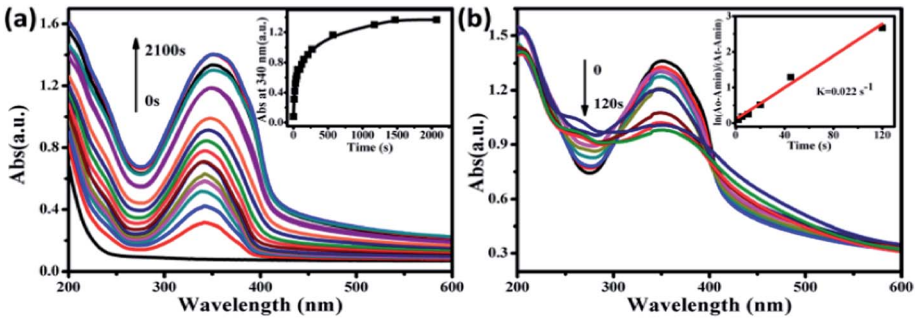

Fig. 2 (a) UV-vis spectra following the infiltration process of DAS into the multilayers; (b) UV-vis spectra of the multilayers following the photochemical reaction of multilayers containing DAS. The inset in panel (a) is the absorbance at 340 nm *versus* the infiltration time. The inset in panel (b) is the value of $\ln\{(A_0 - A_{min})/(A_t - A_{min})\}$ *versus* irradiation time.

and time t, respectively. The surface morphologies of the multilayers were studied using AFM. The substrates before and after DAS infiltration, and that after UV irradiation, exhibited similar surface morphology and surface roughness in the AFM images (Fig. 3). These results indicated that the infiltration process had not destroyed the surface morphology of the multilayers.

After photochemical crosslinking the stability of the multilayers increased significantly. After 30 min immersion in an identical basic solution (pH 12) to that described earlier, no observable change in the appearance of the multilayers could be seen. The UV-vis absorbance spectra after immersion displayed a similar profile to those before immersion, 96% of the intensity being preserved, as shown in Fig. 4(a). AFM measurements on the substrates before and after immersion in the basic solution also showed unchanged surface morphology and roughness (Fig. 4(b) and (c)).

These results were totally different from those of the non-crosslinked multilayers, which disassembled almost completely after immersion in the basic solution for 30 min. These results demonstrated that the crosslinking step is indispensable in obtaining PAH/PAMAM multilayers of satisfactory stability. In addition, the multilayer became more compact on crosslinking, confirmed by a decrease in film thickness from 210 nm to 170 nm (ESI Fig. S1†).

As a further step we studied the influence of crosslinking on the retarded release of the PAH/PAMAM multilayers in 75% aqueous ethanol. It was demonstrated that crosslinking the LbL multilayers containing PAMAM improved the retarded release of the model drug AO from the multilayers. The crosslinked multilayers released this in a retarded manner, and the loading-release performance was highly repeatable. AO was employed as the model drug due to its similarity in structure to drug molecules, and also to its characteristic UV-vis spectra. A solution of ethanol was used for the following three reasons. Firstly, ethanol is a good solvent for AO; secondly, immersion in 75% ethanol is the most widely used sterilization method for biomedical materials; and, finally, the ethanol solution did not disassemble either the non-crosslinked or the crosslinked multilayers within 1 h (ESI Fig. S2†), allowing us to study the release of AO within these films.

Upon immersion in an aqueous solution of AO, both crosslinked and non-crosslinked multilayers absorbed AO. As shown in Fig. 5, the non-crosslinked multilayers absorbed AO quickly during the first 10 min, then slowed down with continued immersion. Finally, the absorption became saturated after 60 min immersion. The crosslinked multilayers, in clear contrast, absorbed AO much more slowly during the first 10 min, the amount of AO absorbed increasing gradually and becoming saturated after 60 min.

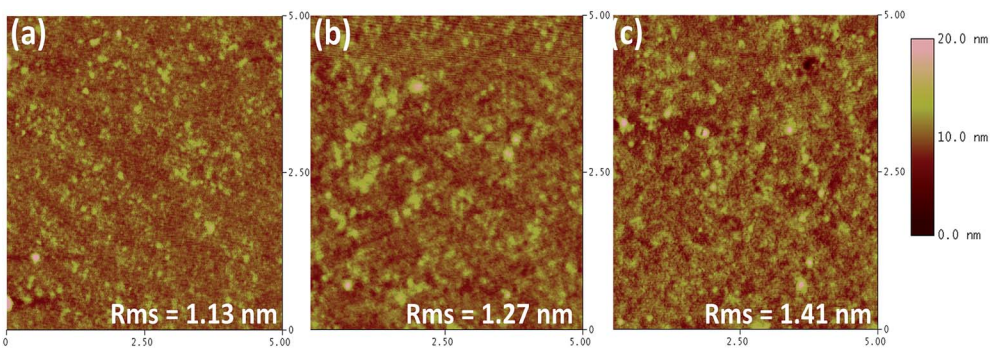

Fig. 3 AFM images of the silica substrate, (a) modified with multilayers $(PAH/PAMAM)_{7.5}$, (b) after post-infiltration of DAS, and (c) following UV irradiation.

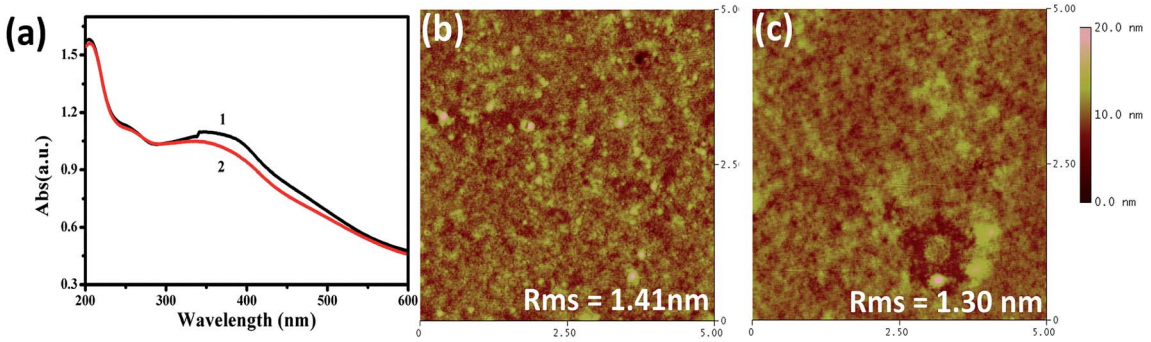

Fig. 4 (a) UV-vis spectra of the crosslinked multilayers before (black) and after (red) immersion in a basic solution at pH 12 for 30 min. AFM images of the surface morphologies of the crosslinked multilayers are shown, (b) before and (c) after 30 min immersion in the basic solution.

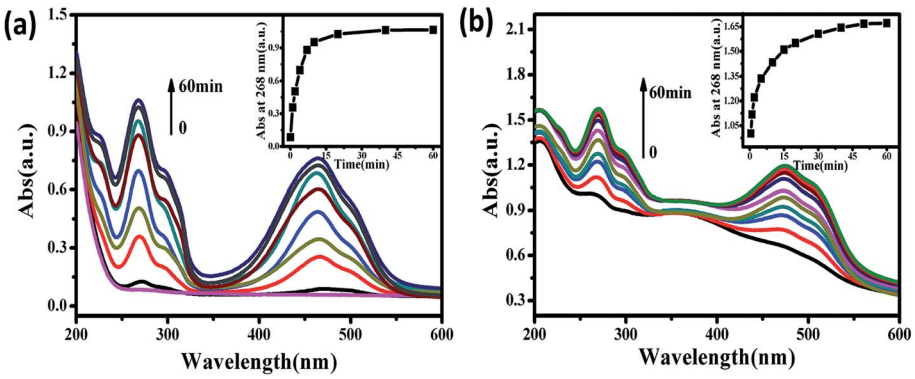

Fig. 5 UV-vis spectra following the infiltration of AO into the (a) non-crosslinked and (b) crosslinked multilayers. The insets in (a) and (b) show the absorbance *versus* infiltration time at 268 nm.

Compared with the non-crosslinked $(PAH/PAMAM)_{7.5}$ multilayer, the corresponding crosslinked multilayer gave a much higher total absorbance, as seen in ESI Fig. S3.† This phenomenon is the result of the absorption of DAS within the multilayer (Fig. 2). After loading the AO molecules, the overall absorption of AO in the cross-linked multilayer was thus very much larger than that in the non-crosslinked multilayer. The loaded concentration of AO was determined after its complete release into solution by reference to a standard UV-vis curve (ESI Fig. S4(a)†). For the crosslinked $(PAH/PAMAM)_{7.5}$ multilayer, the release was slow, and became complete only after about 60 min, when a steady release of 47 μg was found (ESI Fig. S4(b) and (c)†). For the non-crosslinked $(PAH/PAMAM)_{7.5}$ multilayer, total release was complete after about 5 min, when the amount released reached equilibrium at 50 μg (ESI Fig. S4(c)†). The slight difference in the amount of AO loaded suggested that the highly crosslinked $(PAH/PAMAM)_{7.5}$ multilayer had a somewhat lower loading capacity than the non-crosslinked film, due to the compact nature of its structure after crosslinking.

To confirm that AO had been absorbed within rather than on the surface of the multilayer, we investigated the AO release behaviour *versus* the film thickness of the PAH/PAMAM multilayer by controlling the number of bilayers deposited. PAH/PAMAM multilayers were prepared with 2, 4 or 6 bilayers, each being immersed in an aqueous solution of AO dye (0.2 mg mL^{-1}) for 60 min to achieve saturation. The absorbed AO within the multilayer and that released in aqueous solution were tracked using UV-vis spectra (shown in ESI Fig. S5(a) and (b)†). It is seen from the adsorption of the AO dye at 268 nm that an increase in number of bilayers from two to six gave a corresponding increase in the overall absorbance of AO. This suggested that AO was absorbed within the multilayer rather than simply on its surface, since the $(PAH/PAMAM)_2$, $(PAH/PAMAM)_4$ and $(PAH/PAMAM)_6$ multilayers each contained the same PAMAM surface group.

In addition, in order to confirm the necessity of cavity structures within the PAH/PAMAM multilayer formed by the dendritic PAMAM molecule, we adopted a crosslinked PAH/PAA multilayer without noticeable cavity structures as control, and compared the AO absorption behavior of crosslinked $(PAH/PAMAM)_{7.5}$ and $(PAH/PAA)_{7.5}$ multilayers. The results showed that the AO loaded within the crosslinked $(PAH/PAMAM)_{7.5}$ multilayer was almost 3.2 times greater than that within the crosslinked $(PAH/PAA)_{7.5}$ multilayer (ESI Fig. S5c†). This result confirmed that for an identical number of bilayers the PAH/PAMAM multilayer had a higher loading capacity than PAH/PAA, which can be attributed to the cavity structure formed by the highly branched PAMAM molecules.

The release profiles of AO from crosslinked and non-crosslinked multilayers differed significantly, and exhibited similar

trends to their absorption profiles (Fig. 6(a) and (b)). The non-crosslinked multilayers released more than 98% of the AO during the first 5 min. In comparison, the crosslinked multilayers released the AO at a much slower rate – around 95% of the AO was released gradually over a period of 30 min, and saturation was reached only after 60 min. These results confirmed that the non-crosslinked loaded multilayers would not be able to withstand the sterilization process, since small hydrophobic drug molecules, modeled by AO, would almost entirely be lost after 5 min immersion in 75% ethanol. In clear contrast, the crosslinked multilayers retained the AO molecules for a much longer period, and would still be effective as biomedical materials after sterilization.

The slow release of AO from the crosslinked multilayers was likely to have to resulted from their more rigid internal structure after crosslinking, imposing a stronger physical barrier for diffusion of AO both in and out. A sufficiently rigid internal structure of the crosslinked multilayer is believed to be indispensable for obtaining retarded release.

In addition, the loading-release process of the crosslinked multilayers was shown to be repeatable. A constant amount of AO, indicated by the UV-vis spectra, was loaded and released from the crosslinked multilayers over at least 10 cycles with high consistency, as shown in Fig. 6(c). In clear contrast, the loading-release performance of the non-crosslinked multilayers deteriorated rapidly over repeated cycles. After the tenth cycle of the loading-release experiment, only 20% of the quantity loaded in the first cycle was loaded and released, as shown in Fig. 6(d). The rapid deterioration of the performance of the non-crosslinked multilayers is assumed to be the result of relaxation of the internal structure of the multilayers, confirmed by the durability test on the non-crosslinked $(PAH/PAMAM)_{7.5}$ multilayer in the presence of ethanol (ESI Fig. S6(a)†). The results showed that on pre-treating the multilayer with ethanol solution its loading capacity for AO decreased dramatically, indicating that ethanol treatment might to some extent have reduced the loading capacity of the multilayer. In the cycled loading-release experiments, the relaxation of the film structure with the number of cycles performed may be a feature of its decreased loading capacity.

In considering the potential practical applications for drug delivery in aqueous systems, we compared the release behavior of AO in aqueous solutions from non-crosslinked and crosslinked PAH/PAMAM multilayers, respectively. Non-crosslinked and crosslinked $(PAH/PAMAM)_{7.5}$ multilayers were immersed in aqueous solutions of AO (0.2 mg mL^{-1}) for 60 min to achieve saturated absorption. They were each then immersed in water over a series of time intervals and the AO released was tracked by their UV-vis spectra after each time interval. The release process is summarized in Fig. 7. For the non-crosslinked $(PAH/PAMAM)_{7.5}$ multilayer, the absorption of AO molecules within the multilayer fell substantially, to almost zero, after immersing in water for 5 min (Fig. 7(a)). This indicated that AO molecules had been readily released as a result of the concentration gradient between the film and water. In the case of the crosslinked $(PAH/PAMAM)_{7.5}$ multilayer, the release process was

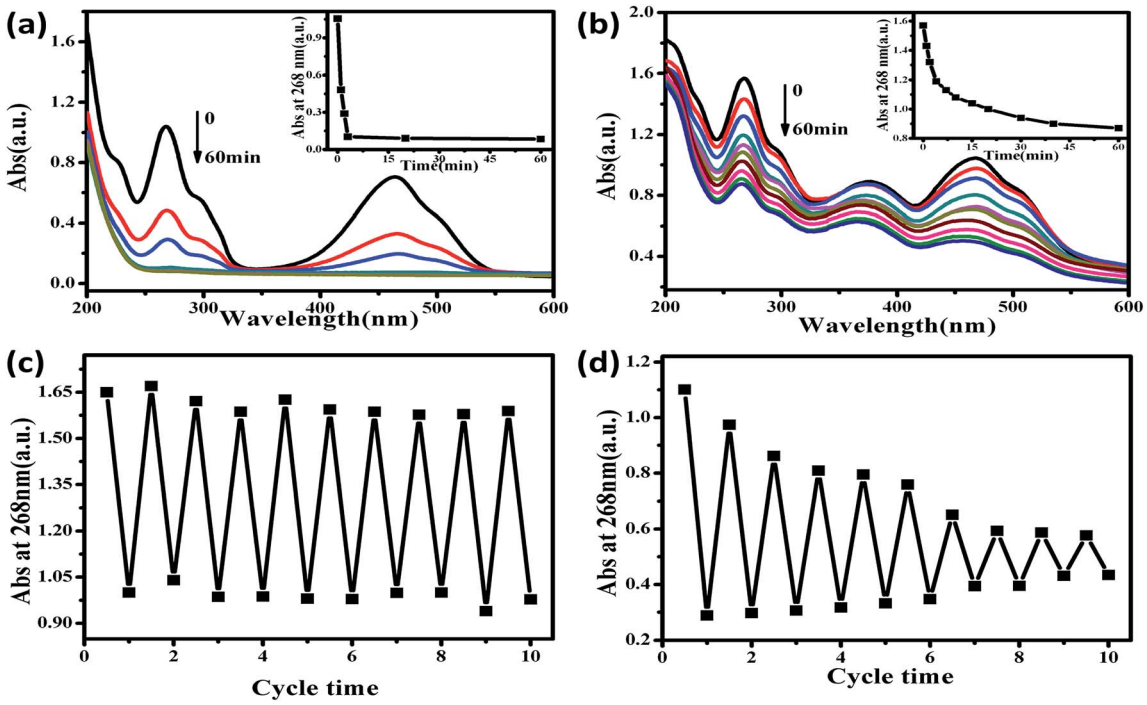

Fig. 6 UV-vis spectra following the release of AO, (a) from non-crosslinked and (b) crosslinked multilayers, and absorbance of the multilayers at 268 nm, corresponding to the maximum absorbance of AO, at saturated infiltration and complete release for (c) crosslinked and (d) non-crosslinked multilayers *versus* cycle number. The insets in panels (a) and (b) show the absorbance of the multilayers at 268 nm *versus* release time.

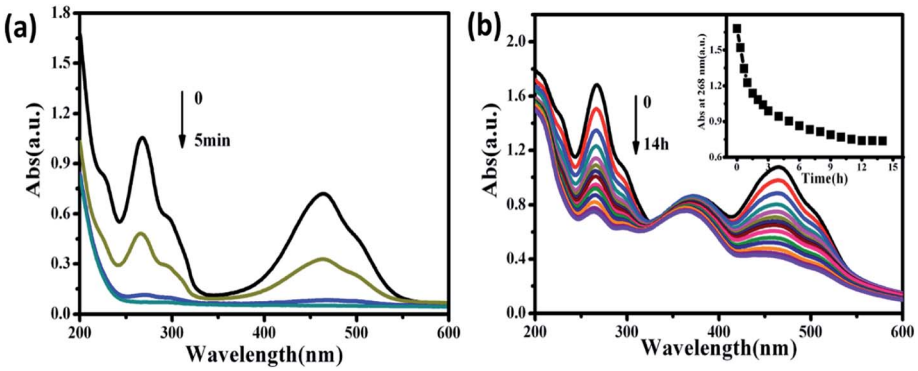

Fig. 7 Release kinetics of AO into water from (a) non-crosslinked and (b) crosslinked $(PAH/PAMAM)_{7.5}$ multilayers.

much slower, as shown in Fig. 7(b). Initially 50% of the loaded AO molecule was released over 3 h, but the release rate was gradually reduced, levelling off to an almost constant value after 12 h. There was hardly any further release of AO during the final 2 h.

These results demonstrated that the crosslinking of the $(PAH/PAMAM)_{7.5}$ multilayer contributed to a covalently connected net of cavity structures, enabling the trapping of small molecules to give slow release of loaded dye molecules. In addition, this slow release behavior in aqueous solution over 12 h shows promise for application to drug delivery systems in future.

4. Conclusions

LbL multilayers with covalently incorporated drug reservoirs were constructed using PAH and PAMAM as building units. A bifunctional photoactive molecule, DAS, was post-infiltrated into the multilayers and produced interlayer crosslinking on UV irradiation. The crosslinked multilayers showed significantly increased stability in a strongly alkaline solution (pH 12). Due to the presence of PAMAM, the multilayers were repeatedly able to load and release the model drug AO with high fidelity. In addition, the multilayers released AO more slowly in 75% ethanol or water, enabling its application as a biomedical material, since this demonstrated that it would withstand the sterilization process. We demonstrated that crosslinking was indispensable in obtaining stable and retarded loading-release performance by the multilayers. We expect the multilayers to find use as functional biomedical materials giving retarded release properties. We also expect the present study to add perspective to the preparation of LbL multilayers offering retarded release of other biologically relevant materials.

Acknowledgements

This work was supported by NSFC (21374006), the Excellent Young Scientist Foundation of NSFC (51422302), the Beijing Natural Science Foundation (2131003), the Program of the Co-construction with Beijing Municipal Commission of Education of China, the Program for New Century Excellent Talents in University (NCET-10-0211), the Fok Ying Tung Education Foundation (131013), the Open Project of the State Key Laboratory of Supramolecular Structure and Materials (SKLSSM201401) and the Beijing Young Talents Plan (YETP0488).

References

1 G. Decher and J. B. Schlenoff, *Multilayer Thin Films*, Wiley-VCH Verlag GmbH & Co. KGaA, Weinheim, Germany, 2003.
2 X. Zhang, *Acta Polym. Sin.*, 2007, **10**, 905.
3 S. Mansouri, F. M. Winnik and M. Tabrizian, *Expert Opin. Drug Delivery*, 2009, **6**, 585.
4 X. H. Liu, J. T. Zhang and D. M. Lynn, *Adv. Mater.*, 2008, **20**, 4148.
5 D. M. Lynn, *Soft Matter*, 2006, **2**, 269.
6 H. Cao, X. Chen, J. R. Yao and Z. Z. Shao, *J. Mater. Sci.*, 2013, **48**, 150.
7 C. Y. Wang, S. Q. Ye, L. Dai, X. X. Liu and Z. Tong, *Biomacromolecules*, 2007, **8**, 1739.
8 A. J. Khopade and F. Caruso, *Langmuir*, 2003, **19**, 6219.
9 J. Choi, T. Konno, M. Takai and K. Ishihara, *Curr. Appl. Phys.*, 2009, **9**, 259.
10 Y. Li, X. Wang and J. Sun, *Chem. Soc. Rev.*, 2012, **41**, 5998.
11 X. Wang, L. B. Zhang, L. Wang, J. Q. Sun and J. C. Shen, *Langmuir*, 2010, **26**, 8187.
12 L. Wang, X. Wang, M. Xu, D. Chen and J. Sun, *Langmuir*, 2008, **24**, 1902.
13 L. Wang, D. D. Chen and J. Q. Sun, *Langmuir*, 2009, **25**, 7990.
14 A. J. Khopade and F. Caruso, *Nano Lett.*, 2002, **2**, 415.
15 A. J. Khopade and F. Caruso, *Langmuir*, 2002, **18**, 7669.
16 Z. L. Liu, X. D. Wang, H. Y. Wu and C. X. Li, *J. Colloid Interface Sci.*, 2005, **287**, 604.
17 J. A. He, R. Valluzzi, K. Yang, T. Dolukhanyan, C. M. Sung, J. Kumar and S. K. Tripathy, *Chem. Mater.*, 1999, **11**, 3268.
18 S. Y. Yang and M. F. Rubner, *J. Am. Chem. Soc.*, 2002, **124**, 2100.
19 K. F. Ren, J. Ji and J. C. Shen, *Bioconjugate Chem.*, 2006, **17**, 77.
20 W. J. Tong, C. Y. Gao and H. Möhwald, *Macromol. Rapid Commun.*, 2006, **27**, 2078.

21 J. Q. Sun, T. Wu, Y. P. Sun, Z. Q. Wang, X. Zhang, J. C. Shen and W. X. Cao, *Chem. Commun.*, 1998, 1853.
22 G. L. Wu, F. Shi, Z. Q. Wang, Z. Liu and X. Zhang, *Langmuir*, 2009, **25**, 2949.
23 J. J. Harris, P. M. DeRose and M. L. Bruening, *J. Am. Chem. Soc.*, 1999, **121**, 1978.
24 J. J. Wu, L. Zhang, Y. X. Wang, Y. H. Long, H. Gao, X. L. Zhang, N. Zhao and J. Xu, *Langmuir*, 2011, **27**, 13684.
25 A. Laschewsky, E. Wischerhoff, P. Bertrand and A. Delcorte, *Macromol. Chem. Phys.*, 1997, **198**, 3239.
26 P. Urban, J. J. Valle-Delgado, N. Mauro, J. Marques, A. Manfredi, M. Rottmann, E. Ranucci, P. Ferruti and X. Fernandez-Busquets, *J. Controlled Release*, 2014, **177**, 84.
27 S. Mignani, S. El Kazzouli, M. Bousmina and J. P. Majoral, *Adv. Drug Delivery Rev.*, 2013, **65**, 1316.
28 P. Kesharwani, K. Jain and N. K. Jain, *Prog. Polym. Sci.*, 2014, **39**, 268.
29 J. Zhu and X. Shi, *J. Mater. Chem. B*, 2013, **1**, 4199.
30 K. Sato and J. I. Anzai, *Molecules*, 2013, **18**, 8440.
31 S. Tomita, K. Sato and J. I. Anzai, *J. Colloid Interface Sci.*, 2008, **326**, 35.
32 C. Park, M. Rhue, M. Im and C. Kim, *Macromol. Res.*, 2007, **15**, 688.
33 S. R. Puniredd and M. P. Srinivasan, *J. Colloid Interface Sci.*, 2007, **306**, 118.
34 H. Li, Z. Li, L. Wu, Y. Zhang, M. Yu and L. Wei, *Langmuir*, 2013, **29**, 3943.
35 K. M. Gattás-Asfura and C. L. Stabler, *ACS Appl. Mater. Interfaces*, 2013, **5**, 9964.
36 C. P. Silva and H. M. Carapuca, *Electrochim. Acta*, 2006, **52**, 1186.
37 X. S. Zhang, C. Jiang, M. J. Cheng, Y. Zhou, X. Q. Zhu, J. Nie, Y. J. Zhang, Q. An and F. Shi, *Langmuir*, 2012, **28**, 7096.
38 Y. Zhou, M. Cheng, X. Zhu, Y. Zhang, Q. An and F. Shi, *J. Mater. Chem. A*, 2013, **1**, 11329.
39 Y. Zhou, M. Cheng, X. Zhu, Y. Zhang, Q. An and F. Shi, *ACS Appl. Mater. Interfaces*, 2013, **5**, 8308.
40 Q. An, Y. Zhou, Y. Zhang, Y. Zhang and F. Shi, *RSC Adv.*, 2014, **4**, 5683.